

The Effects of Dynamic Saddle Annulus and Leaflet Length on Transmitral Flow Pattern and Leaflet Stress of a Bileaflet Bioprosthetic Mitral Valve

Arash Kheradvar, Ahmad Falahatpisheh

The Edwards Lifesciences Center for Advanced Cardiovascular Technology, The Henry Samueli School of Engineering, University of California, Irvine, Irvine, CA, USA

Background and aim of the study: The study aim was to determine the effect of mitral saddle annulus and leaflet length on peak leaflet stress and transmitral flow pattern when utilizing a novel bileaflet bioprosthetic valve.

Methods: A novel valve, which closely mimics the saddle annulus motion of the mitral valve was developed. A series of computational analyses and in-vitro hemodynamic studies was performed to assess the effect of annulus dynamics and leaflet length on stress distribution at the leaflet tips as well as the transmitral flow pattern downstream of the valve.

Results: The analysis showed that the dynamic annulus may significantly reduce stress along the tip of the leaflets compared to the rigid annulus in a standard trileaflet valve. The leaflet length may also significantly alter stress distribution over the leaflets

by affecting the annulus dynamics. It was shown in vitro that the interaction between the leaflet and the ventricular results in fundamentally distinct transmitral vortex formation patterns.

Conclusion: Motion of the mitral saddle annulus along with the leaflet length is a critical factor that minimizes stress distribution at the tips of the leaflets due to a dampening of the pressure load exerted over the valve during the cardiac cycle. The length of the leaflets, and their proximity to the ventricular wall, have been shown to have significant effects on transmitral vortex formation and energy dissipation during blood transfer from the left atrium towards the aorta via left ventricle.

The Journal of Heart Valve Disease 2012;21:225-233

Mitral valve is a unique valvular structure whose number of leaflets and saddle shape of its annulus make it distinct from the other three valves inside the heart. Currently, there is no firm evidence why a bileaflet structure having developed in the mitral position compared to trileaflet structures in other heart valves. One hypothesis is based on the potential advantages of an asymmetric vortex bubble (1-3) and an elliptical flow profile that forms through a bileaflet valve, compared to the symmetric, round vortex bubble that develops through a trileaflet valve (2, 4-6). The results of previous studies have shown that the deflecting saddle shape of the valve's annulus may

Parts of this manuscript have been selected for presentation at the 2010 Scientific Session of the American Heart Association and the 6th Biennial Meeting of The Society for Heart Valve Disease to be held in Barcelona on the 25-28 June 2011

Address for correspondence:

Arash Kheradvar MD, PhD, The Edwards Lifesciences Center for Advanced Cardiovascular Technology, The Henry Samueli School of Engineering, University of California, Irvine, 24010 Engineering Hall, Irvine, CA 92697, USA
e-mail: arashkh@uci.edu

also improve the transmitral momentum transfer from the left atrium towards the aorta, through the left ventricle (7-9). Nevertheless, there is an overall agreement that the saddle-shape annulus of the mitral valve is a critical component of the left heart complex, the contribution of which in creating efficient valve closure and robust ventricular filling is unquestioned (10-14).

The dynamic nature of mitral annulus motion has been verified previously in humans (15, 16) and in animal models (11, 12). For example, Carlhäll et al. (10) showed that the excursion of the mitral annulus significantly accounted for the total left ventricular filling and emptying in humans. This situation arises mainly because the annulus plays a sphincter-like role when facilitating ventricular filling and valve closure during diastole and systole, respectively. In addition, the geometry of the mitral annulus has been shown to be a significant parameter in the diagnosis of functional disorders such as mitral valve prolapse, functional mitral regurgitation (17) and acute ischemic

mitral regurgitation (18-20). The mitral valve is a major contributor of the ventricular flow pattern, which is extremely critical with respect to momentum transfer, energy dissipation (3, 21) and the pumping efficiency of the left ventricle (7, 9, 22-26).

While the unique characteristics of the mitral valve have been extensively identified and studied during recent years, none of these has been incorporated into the development of mitral valve prostheses. Consequently, a bileaflet mitral bioprosthetic was developed by the present authors (27) that mimics the motion of the mitral valve's saddle annulus.

The aim of the present study was to examine the effect of the dynamic saddle annulus on transmural flow and stress distribution among the leaflets, by exploiting the bileaflet bioprosthetic mitral valve.

Materials and methods

Bioprosthetic design

The dynamic motion of the natural mitral valve is due to the elastic composition of its fibrous annulus (28). To imitate the motion of the mitral annulus, superelastic Nitinol wires were used with 8% strain recovery, shaped into a saddle-shape annulus with two prongs for attachment and holding the leaflets. The annulus was sutured to the proximal ends of the leaflets, which were made from bovine pericardial tissue. The leaflets and the saddle-shaped annulus

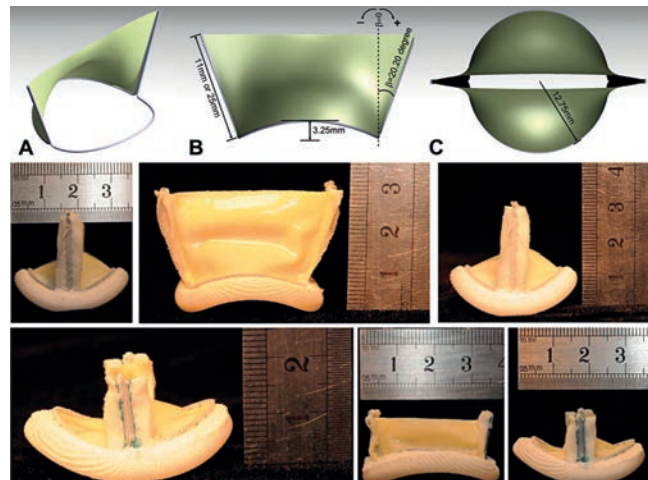


Figure 1. Bi-leaflet mitral bioprosthetic with saddle shape annulus. Top: (A) mid-section of the valve showing the Nitinol core surrounded by pericardial tissue; (B) Bioprosthetic valve in open configuration from convex side. The valve dimensions and the angle of motion are shown; (C) schematic from the top when the valve is fully open; Middle: bioprosthetic valve with 25mm leaflet length; Bottom: bioprosthetic valve with 11mm leaflet length. The leaflets are made of bovine pericardial tissue with an average thickness of 0.5mm.

were also sutured to each other by means of two Nitinol supporting prongs that extended from the annulus alongside the leaflets (Fig. 1). The supporting prongs act in similar fashion to the chordae tendineae, preventing the leaflets from being prolapsed toward the atrium (Fig. 1). The valve characteristics, such as annulus height, curvature and the critical prong angle, were optimized by constraining the Nitinol wire to a specialized housing unit designed for an adult heart with an annulus diameter of 25 mm. The dimensions of the bioprosthetic valve are shown in Figure 1.

Computational Modeling

To computationally model the stress distribution over the valve leaflets, the solid geometry of the Nitinol framework and the leaflets were independently developed (Fig. 1, top) and imported into a computational analysis software environment. CATIA (Dassault Systèmes, Lowell, MA, USA), and ABAQUS (SIMULIA, Warwick, RI, USA) were utilized for mechanical design and computational analysis, respectively. The Nitinol construct was modeled based on the Ogden strain energy function (29), which has been found to accurately fit to the present experimental uniaxial tension test for Nitinol wires. The constitutive model for mitral leaflets was adopted from May-Newman and Yin (30)

$$\psi(I_1, I_4) = \bar{c}_0 [\exp(\bar{c}_1(I_1 - 3)^2 + \bar{c}_2(\sqrt{I_4} - 1)^4) - 1] \quad (1)$$

where ψ is the strain-energy function, and c_i ($i = 0, 1, 2$) are the independent material constants that characterize the deviatoric deformation of the leaflet material (31). The tissue material model was applied using the UMAT user subroutine in ABAQUS. The constitutive model (30) took into account the dependency of the strain energy function on fiber direction of the leaflet through the fourth pseudoinvariant of right Cauchy-Green deformation tensor (I_4). Therefore, the components of stiffness matrix were dependent on the derivative of the strain energy and the fiber direction, defining a transversely isotropic material behavior for the leaflets.

The leaflets and Nitinol structure were assembled to ensure the consistency and uniformity of the valve model. Linear triangular shell elements were used for the leaflets, linear hexahedral elements for the Nitinol, and linear quadrilateral elements for the discrete rigid surfaces, which defined the contact boundary conditions at the coaptation regions. A static pressure was imposed as a ramp over the tissue mesh to close the leaflets.

To compare the stress distribution over the bileaflet valves with the standard trileaflet valve, a trileaflet valve with 25 mm diameter and a rigid annulus was

modeled using CATIA with a leaflet length of 12.4 mm. Similar computational methodology and boundary conditions (as described earlier) were applied to the trileaflet valve to obtain the stress distribution over the leaflets.

In-vitro hemodynamic study

The experimental set-up utilized in study (32) comprised a thin-walled ventricle, shaped according to the systolic state, and made from transparent silicone rubber. The ventricular sac was suspended over the Plexiglas atrium free-floating inside a rigid, water-filled, cubic container made from Plexiglas that was connected to a hydraulic pump system (Superpump system; Vivitro Systems Inc., Victoria, BC, Canada). The pump was controlled by a customized interface that regulated the motion of the pump's piston according to predefined waveforms (32) and which were automatically adjusted based on the position, velocity and pressure feedback received by the power amplifier (SPA3891Z; Vivitro Systems Inc.). The waveforms induced the desired transmural suction and transaortic forward flow in the silicone ventricle during the cardiac cycle.

Valve placement

The bileaflet mitral prototypes and the control trileaflet valve (SJM Biocor™; St. Jude Medical, Inc., MN, USA) were placed at the mitral position, and a 23 mm Sorin Biomedica Carbocast mechanical heart valve (CarboMedics, Austin, TX, USA) was placed at the aortic position. Distilled water was used as the circulating fluid.

To reproduce the cardiac cycle, a waveform that creates a systolic ratio (SR) of 40% was used to imitate the ventricular flow conditions. The SR is the fraction of time in a cardiac cycle during which the left ventricle is in systolic phase (32). The frequency of cycles was set to different values ranging from 1 Hz to 1.67 Hz (60-100 beats per min) to reproduce an operational range for cardiac function. Each experiment was set to run for 10 s (10-16 cardiac cycles) to ensure the consistency and reproducibility of the results. The atrial contraction phase was not reproduced by this waveform.

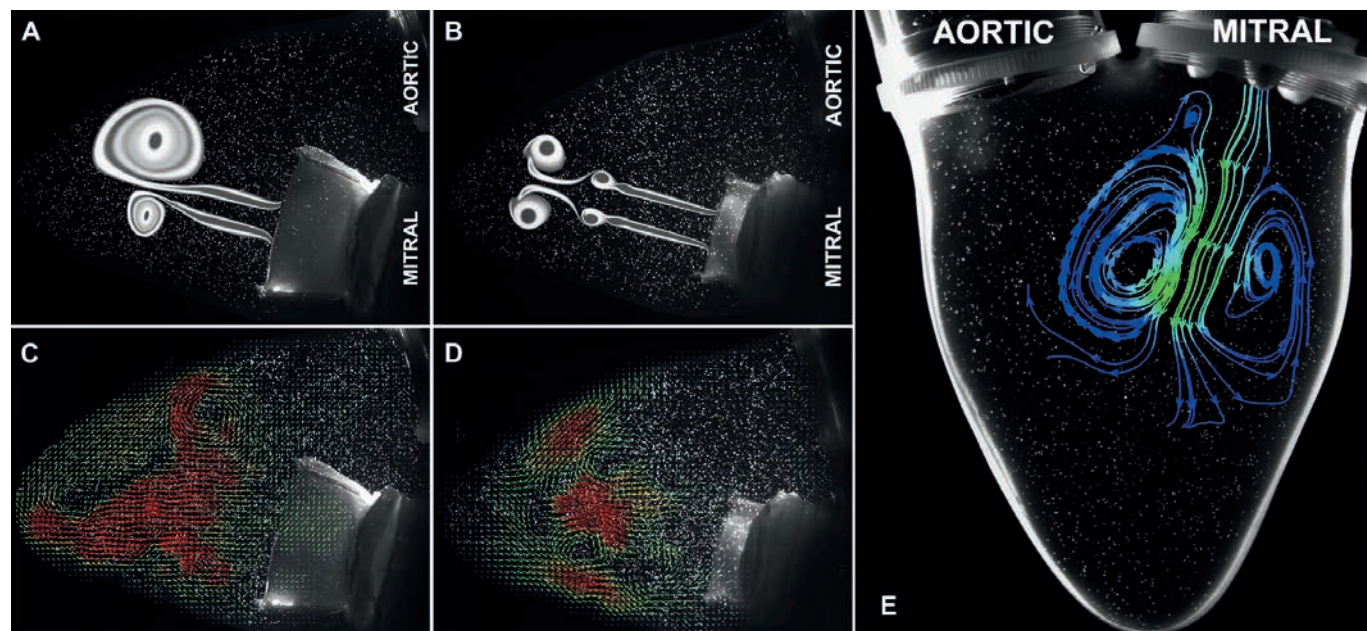


Figure 2. (A) vortex formation downstream the valve with 25mm leaflet length. An asymmetric, unstable vortex is formed. (B) shows the vortex formation downstream the valve with 11mm leaflet length. A symmetric, stable vortex is formed. (C) Velocity vector field obtained from DPIV at mid-diastole downstream the valve with 25mm leaflet length. Asymmetric circulatory pattern of transmural jet can be observed. (D) Velocity vector field obtained from DPIV at mid-diastole downstream the valve with 11mm leaflet length. Symmetric circulatory pattern of transmural jet can be observed; (E) Streamlines of transmural jet downstream a 25mm Mitral Biocor™ by St. Jude Medical is obtained using DPIV. The leading symmetrical vortex ring in front of the jet can be observed.

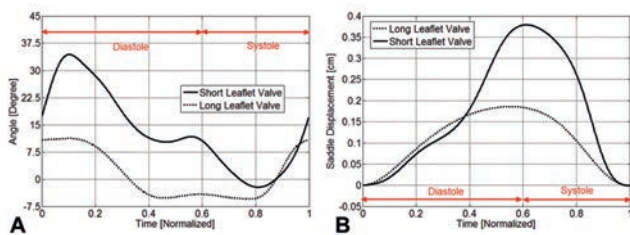


Figure 3. Annulus dynamics. (A) The angle of motion for the supporting prongs during a cardiac cycle for both valves; (B) Displacement at the tip of saddle annulus during a cardiac cycle; positive direction is toward increasing the saddle convexity.

Measurement methods

The flow characteristic information and the valves' dynamics were measured using digital particle image velocimetry (DPIV) and image processing tools.

Flow visualization

DPIV uses two digital images of a particle-seeded flow illuminated by a thin laser sheet to determine the displacement field of the particles in the field of view by cross-correlating pixels in a subsection of two images. The flow was seeded with neutrally buoyant, orange fluorescent particles with a diameter in the range of 60–80 µm (32). A high-speed digital camera (1030 fps, 1280 × 1024; Y3, IDTVision, Inc.) was used in the ventricular chamber to capture the image sequences of the particle field. Pairs of images were captured from an illuminated sheet of fluorescent particles generated by a double-pulsed Nd:YLF green pump laser (Coherent, Inc., Santa Clara, CA, USA). This system enabled the capture of 1000 velocity frames per second, which guaranteed an accurate mapping of the flow downstream of the valve.

Annulus dynamics

The motion of the bileaflet valves' annulus was captured during the cardiac cycle through high-speed imaging (1030 fps; 1280 × 1024). The tip of the saddle's movement and the angle of motion of the prongs were measured based on tracking the objects using the image-processing toolbox of MATLAB (MathWorks, Inc.).

Statistical analysis

All statistical analyses were performed using MATLAB (Mathworks, Inc.). Differences among the groups were tested for significance using an unbalanced one-way analysis of variance (ANOVA), with subgroup analysis by the Scheffé F-test. A p-value <0.05 was considered to be statistically significant.

Results

Velocity fields of transmural flow:

Flow fields downstream of each valve were mapped using DPIV. The velocity vectors overlaid on the particle field of the bileaflet valves are shown in Figure 2; the schematic of transmural vortex formation downstream of the short-leaflet and long-leaflet valves are shown in Figures 2A and 2B, respectively. The velocity vector fields at mid-diastole for both valves are shown in Figures 2C and 2D, respectively. A symmetric vortex was observed downstream of the mitral valve with short leaflets, while an asymmetric, unstable vortex was developed by the mitral valve with long leaflets, despite the identical cardiac cycles, pressure drop, afterload and the preload in both cases. Flow downstream of the standard trileaflet valve at the mitral position was also mapped using high-speed DPIV. The streamlines that defined the flow field were overlaid on the particle field (Fig. 2E); a symmetric vortex, forming along with the transmural jet, was observed during diastole.

Annulus dynamics

Elastic deformation of the saddle-shaped annulus was captured through high-speed imaging, and analyzed using image-processing tools. When the valve was opening during diastole (Fig. 3), the saddle annulus demonstrated a convex shape at the sides, while the supporting prongs were curved appropriately outwards, keeping the leaflets far from each other and maintaining the utmost orifice size (Fig. 1). When the valve was closed during systole, the saddle annulus was deflected back to a less convex or even flat shape, while the supporting prongs became curved inwards so as to minimize the orifice and prevent regurgitation.

The angle of motion (β) for the supporting prongs is defined in Figure 1B. When the valve was in the fully relaxed mode (i.e., partially open), the angle β was +20.20° and +11.25° for the short-leaflet and long-leaflet valves, respectively. During systole, the distal end of the prongs began to move towards the center of the valve, and this resulted in smaller values of β . When the tip of a prong passed the imaginary line at the intersection of the annulus saddle and the prongs, the angle β turned negative according to the sign convention (Fig. 1B). Based on these experiments, the angle of motion changed in the range of -3 to 35° and -5 to 11.25° in the short-leaflet and long-leaflet valves, respectively (Fig. 3). During systole, the saddle tips of both valves underwent axial displacement, changing from a convex to a flat shape (Fig. 1B). The maximum displacements of the saddle tip for the short-leaflet and long-leaflet valves were 3.85 mm and 3.65 mm, respectively (Fig. 3).

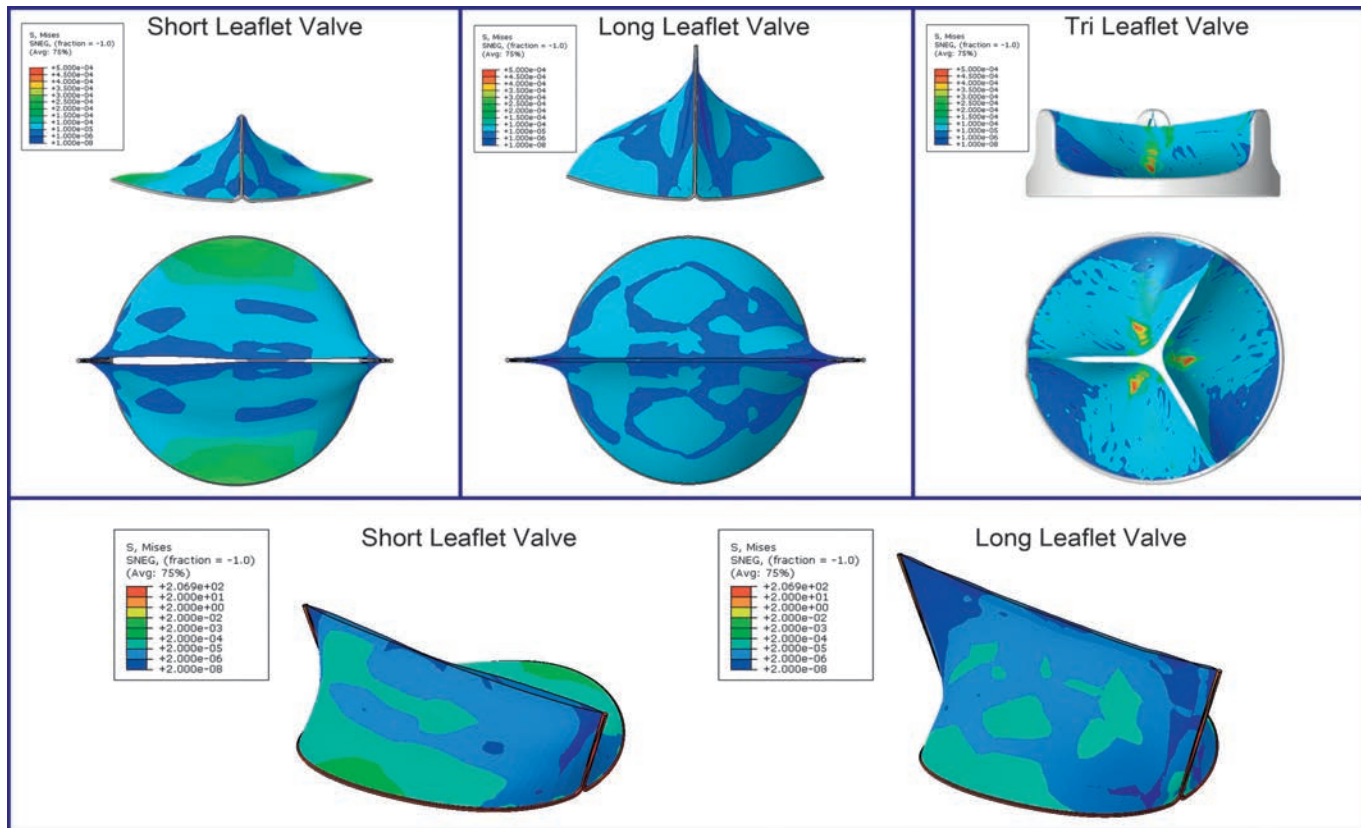


Figure 4. Stress distribution over the leaflets at the valve closure: (Top) compares the Von Mises stress distribution over the leaflets of the studied valves; (Bottom) higher concentration of stress is developed over the saddle-shape annulus compared to leaflets in bileaflet valves.

Leaflet stress distribution

The finite element analyses performed were based on applying a pressure boundary condition as a ramp for closure of the leaflets. According to the mesh sensitivity analysis, the number of elements in each dimension for each valve model was doubled, with 12,000 and 4,000 elements, respectively, being used to ensure the mesh independency of the results. The Von Mises stress data showed a complete resemblance between both cases. The stress distribution was slightly different due to the number of elements, which showed about a 5% discrepancy.

The stress distributions over the valves are presented in Figures 4 and 5, and Tables I and II. The Von Mises

stresses that were computed along the tip of the leaflet and at the leaflet symmetry line are listed in Table I.

In Figure 4, the range of the stress has been set equal for all three valves, to facilitate the comparison. The red areas were considered high stress concentration zones, which were only present in the trileaflet valve. In the bileaflet valves, the Von Mises stress distributions implied that the inplane stress at the leaflet tips was substantially smaller than in the remainder of the valve, regardless of the leaflet length, and in contradistinction to the trileaflet valve with a rigid annulus (Fig. 4).

The comparison of stress distribution along the tip and at the symmetry line of the leaflet among the

Table I: Von Mises stress distribution.

	Long bileaflet valve	Short bileaflet valve	Trileaflet valve
Number of stress data points			
Along the tip of leaflet	56	48	101
At the symmetry line	27	16	55
Magnitude (Pa)			
Along the tip of leaflet	0.0017 ± 0.0016	0.0034 ± 0.0030	0.0642 ± 0.0608
At the symmetry line	0.0218 ± 0.0143	0.0711 ± 0.0882	0.0976 ± 0.0964

Table II: Von Mises stress' statistics

	F-Statistics	P-value	Significance
Stress along the tip of the leaflet (all three valves)	53.25	0.0000	S
Stress at the symmetry line (all three valves)	7.93	0.0006	S
Stress along the tip (short and long bileaflet valves)	12.78	0.0005	S
Stress at the symmetry line (short and long bileaflet valves)	8.23	0.0064	S
Stress along the tip (long and trileaflet valves)	58.95	0.0000	S
Stress at the symmetry line (long and trileaflet valves)	16.42	0.0001	S
Stress along the tip (short and trileaflet valves)	47.79	0.0000	S
Stress at the symmetry line (short and trileaflet valves)	0.97	0.3289	NS

S: Significant; NS: Not significant.

valves is shown as box plots in Figure 5. In Figure 5A, the stress distribution along the leaflet tip was shown to be significantly higher ($p < 0.0001$; Table II) in the trileaflet valve (0.0642 ± 0.0608 Pa) compared to the other two valves (0.0017 ± 0.0016 Pa and 0.0034 ± 0.0030 Pa, respectively; Table I). The stress distribution at the symmetry line of the leaflet was also significantly different among the three valves (Fig. 5B; Table II). Considering the two bileaflet prototypes, the leaflet stress - both along the tip ($p < 0.0001$) and at the symmetry line ($p < 0.0064$) - was smaller in the longleaflet valve compared to the short-leaflet valve (Table II; Fig. 5C and D).

Discussion

A novel mitral bioprosthetic valve with a dynamic saddle-shaped annulus has been developed that

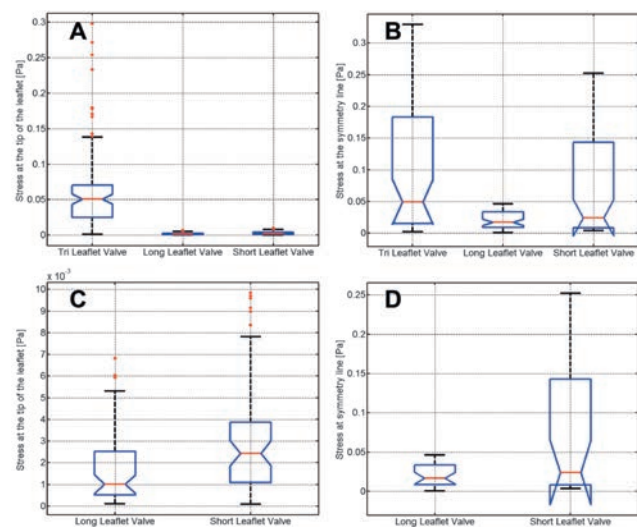


Figure 5. Box plots of leaflet stress among the studied valves. (A) the stress distribution along the tip of leaflet among all three valves; (B) The stress distribution at the symmetry line of the leaflet among the three valves; (C) the stress distribution along the tip of leaflet of bileaflet valves; (D) the stress distribution at the symmetry line of leaflet of bileaflet valves.

mimics the natural motion of the mitral valve. By comparing two prototypes of this valve with each other, and also with a standard trileaflet valve, investigations were made as to how motion of the annulus and the valve geometry would affect stress distribution over the leaflets, and the transmural flow pattern. The leaflet lengths selected for the bileaflet valve - 25 and 11 mm - were two extreme cases based on data available for the anatomy of the mitral valve. Klues et al. (33) reported the anterior leaflet length as 19 ± 4.0 mm and 22 ± 5.0 mm in patients with normal and enlarged actual mitral leaflet areas, respectively, while Timek et al. (34) showed the length of the anterior and posterior leaflets in sheep to be in the range of 21.1 ± 1.6 mm and 11.4 ± 2.7 mm, respectively.

Transmural Vortex Formation

Previously, it has been confirmed in several studies that vortical flow structures develop along with the strong propulsive transmural jet (1, 5, 6, 22, 35). However, there is currently no firm agreement on the shape and rotational direction of the vortex structures that develop along with the normal transmural flow. Recent studies have indicated that in a normal heart, due to the asymmetry of the leaflets, the transmural vortex tends to be more asymmetric (1, 3). Based on data acquired from current in-vitro studies, changes in mitral leaflet length can greatly affect transmural vortex formation due to an altered flow-wall interaction. Similar results for vortex dynamics have been reported under different conditions involving flow-wall interactions (6, 36). The data obtained in the present study also showed that the transmural vortex formation could be influenced by the saddle annulus dynamics, and also by the angle of valve opening.

As shown in Figure 2, a symmetric, donut-shaped vortex ring was formed along with the transmural jet downstream of the mitral valve with a leaflet height of 11 mm. However, increasing the leaflet length to 25 mm resulted in an asymmetric, unstable leading vortex along with the transmural jet. It might be speculated that flow interaction with the ventricular

sac would significantly influence the stability, dynamics and shape of the leading vortex that develops along with transmural jet. The flow-wall interaction phenomenon exists in vivo, depending on the distance between the tip of the natural mitral valve's leaflet and the ventricular wall.

For comparative purposes, the flow downstream of a standard trileaflet porcine valve (SJM Biocor) was also mapped. In this case, the formed vortex was entirely symmetric (Fig. 2E), due to the arrangement of the three leaflets that create a circular orifice when the valve is open, and the short leaflet length (9–10 mm) that prevents any interaction with the walls. A similar observation has also been reported previously for pericardial trileaflet valves (37).

In normal hearts, the leading vortex transfers extra momentum from the left atrium to the left ventricle, thus contributing to an efficient transport of blood towards the aorta. The additional sources of momentum-transfer derive either from the added mass effect (38), in which the streamlines act as a boundary that drives the ambient fluid into motion when the vortex is being formed, or from fluid entrainment inside the isolated transmural vortex bubble (39). Accordingly, some of the residual blood inside the left ventricle ahead of the transmural jet is accelerated forwards while the transmural jet is being initiated. At the same time, some ambient fluid must be brought in behind the vortex ring so as to preserve the continuity of the flow. The proximity of the leaflet tip to the ventricular wall will significantly affect the process of vortex formation (36), and the flow pattern observed downstream of the bileaflet prototype with longer leaflets may be closer to reality.

Mitral Annulus Dynamics

The saddle dynamics during the cardiac cycle is shown in Figure 3. It was observed that the shortleaflet valve demonstrated an additional recoil in response to certain pressure fields when compared to the long-leaflet valve. The displacement of the saddle annulus and the prong's angle of motion were significantly larger in the short-leaflet prototype.

Stress distribution over the leaflet

The computational results showed that stress distribution at the leaflet tips during systole were overall much smaller than the stress generated over the annulus in the bileaflet prototypes (Fig. 5; Table I). The stress distribution over the leaflet builds up gradually as it approaches the annulus, an effect which is due to the deformability of the annulus in these valves, as the stress is concentrated over the annulus. The deflection of the mitral annulus during valve opening and closure considerably dampens the load

exerted over the valve. As a result, the annulus motion prevents the leaflet from being exposed to excessive tensile stress as most of the load is carried by the annulus itself – as evidenced by the Von Mises stress, the magnitude of which is greater around the annulus (Fig. 4). The stress at the leaflet tip and at the line of leaflet symmetry was higher in the short-leaflet valve than in the long-leaflet valve (Table II; Fig. 5C and D). Considering that the short-leaflet prototype undergoes a higher rate of recoil (as shown in Fig. 3), a higher level of stress can be anticipated. Consequently, it is to be expected that an optimal leaflet length per annulus diameter size may result in a desired annulus dynamic with minimal stress distribution over the leaflets.

A comparison between the bileaflet and trileaflet valves showed that the tip of the trileaflet valve leaflets with a rigid annulus underwent greater Von Mises stress (Table I) when subjected to the same boundary and initial conditions. This is illustrated in Figure 4 (top row), where the red areas that represent high stress concentration zones are present only in the trileaflet valve. According to the computational analyses, the magnitude of stress developed along the leaflet tips of the trileaflet valve was significantly higher than that of the bileaflet valves.

The magnitude of stress at the leaflet's symmetry line was not found to differ significantly between the trileaflet and bileaflet valves with short leaflets (Table II; Fig. 5B), an observation which highlighted the effect of leaflet length on leaflet stress distribution. The trileaflet and short-bileaflet valves possessed leaflets of about the same length (11 mm and 12.4 mm, respectively). When the leaflets are very short, an elastic deformation of the mitral annulus may have a minimal influence on damping the stress over the leaflet area. Nevertheless, the dynamic annulus reduces the stress at the tip of the leaflet, regardless of leaflet length (Tables I and II; Figs. 4 and 5).

Study limitations

The primary limitation was that these mitral bioprostheses have not yet been implanted in a living heart. Although the mitral leaflet length could be varied from 11 to 25 mm, based on left ventricular size (33, 34), the optimal length of the leaflets should be defined based on data acquired from animal studies. Shortening the leaflets beyond 11 mm may lead to an incomplete leaflet coaptation, regurgitation, or even valve prolapse, whereas lengthening the leaflets beyond 25 mm may result in interference with the chordae tendineae and left ventricular outflow tract obstruction. A further limitation was that distilled water was employed as the circulating fluid, but the higher viscosity of blood may affect the transmural flow, by increasing the dissipation.

In conclusion, the results obtained suggest that the leaflet dimensions and dynamic structure of the mitral valve annulus are critically important, and may significantly influence stress distribution over the leaflets. Clearly, these geometric relationships should be taken into account when designing and developing mitral valve bioprostheses, as the achievement of lower stress values at the leaflet tip would not only minimize the risk of calcification but also prolong the operational lifetime of the valve.

Acknowledgement

These studies were supported by American Heart Association Grant No. 10BGIA4170011.

References

1. Kheradvar A, Houle H, Pedrizzetti G, Tonti G, Belcik T, Ashraf M, et al. Echocardiographic Particle Image Velocimetry: A Novel Technique for Quantification of Left Ventricular Blood Vorticity Pattern. *J Am Soc Echocardiogr.* 2010;23:86-94
2. Pasipoularides A, Shu M, Shah A, Womack MS, Glower DD. Diastolic right ventricular filling vortex in normal and volume overload states. *Am J Physiol Heart Circ Physiol.* 2003;284:H1064-1072
3. Kheradvar A, Assadi R, Falahatpisheh A, Sengupta PP. Assessment of Transmural Vortex Formation in Patients with Diastolic Dysfunction. *Journal of the American Society of Echocardiography.* 2012;25:220-227
4. Kheradvar A, Gharib M. Influence of Ventricular Pressure Drop on Mitral Annulus Dynamics Through the Process of Vortex Ring Formation. *Ann Biomed Eng.* 2007;35:2050-2064
5. Kheradvar A, Gharib M. On Mitral Valve Dynamics and its Connection to Early Diastolic Flow. *Ann Biomed Eng.* 2009;37:1-13
6. Kheradvar A, Milano M, Gharib M. Correlation between vortex ring formation and mitral annulus dynamics during ventricular rapid filling. *ASAIO J.* 2007;53:8-16
7. Jiamsripong P, Calleja AM, Alharthi MS, Dzsinich M, McMahon EM, Heys JJ, et al. Impact of Acute Moderate Elevation in Left Ventricular Afterload on Diastolic Transmural Flow Efficiency: Analysis by Vortex Formation Time. *J Am Soc Echocardiogr.* 2009;22:427-431
8. Pedrizzetti G, Domenichini F. Nature Optimizes the Swirling Flow in the Human Left Ventricle. *Phys Rev Lett.* 2005;95:108-101
9. Sengupta PP, Tajik AJ, Chandrasekaran K, Khandheria BK. Twist Mechanics of the Left Ventricle: Principles and Application. *J Am Coll Cardiol Img.* 2008;1:366-376
10. Carlhall C, Wigstrom L, Heiberg E, Karlsson M, Bolger AF, Nylander E. Contribution of mitral annular excursion and shape dynamics to total left ventricular volume change. *Am J Physiol Heart Circ Physiol.* 2004;287:H1836-841
11. Karlsson MO, Glasson JR, Bolger AF, Daughters GT, Komeda M, Foppiano LE, et al. Mitral valve opening in the ovine heart. *Am J Physiol Heart Circ Physiol.* 1998;274:H552-563
12. Salgo IS, Gorman JH, III, Gorman RC, Jackson BM, Bowen FW, Plappert T, et al. Effect of Annular Shape on Leaflet Curvature in Reducing Mitral Leaflet Stress. *Circulation.* 2002;106:711-717
13. Timek TA, Lai DT, Dagum P, Tibayan F, Daughters GT, Liang D, et al. Ablation of mitral annular and leaflet muscle: effects on annular and leaflet dynamics. *Am J Physiol Heart Circ Physiol.* 2003;285:H1668-674
14. Timek TA, Miller DC. Experimental and clinical assessment of mitral annular area and dynamics: what are we actually measuring? *Ann Thorac Surg.* 2001;72:966-974
15. Jimenez JH, Soerensen DD, He Z, He S, Yoganathan AP. Effects of a Saddle Shaped Annulus on Mitral Valve Function and Chordal Force Distribution: An In Vitro Study. *Ann Biomed Eng.* 2003;31:1171-1181
16. Ryan LP, Jackson BM, Enomoto Y, Parish L, Plappert TJ, St. John-Sutton MG, et al. Description of regional mitral annular nonplanarity in healthy human subjects: A novel methodology. *J Thorac Cardiovasc Surg.* 2007;134:644-648
17. Aikawa K, Sheehan FH, Otto CM, Coady K, Bashein G, Bolson EL. The severity of functional mitral regurgitation depends on the shape of the mitral apparatus: a three-dimensional echo analysis. *J Heart Valve Dis.* 2002;11:627-636
18. Glasson JR, Komeda M, Daughters GT, II, Bolger AF, MacIsaac A, Oesterle SN, et al. Three-Dimensional Dynamics of the Canine Mitral Annulus During Ischemic Mitral Regurgitation. *Ann Thorac Surg.* 1996;62:1059-1067
19. Gorman JH, III, Gorman RC, Jackson BM, Hiramatsu Y, Gikakis N, Kelley ST, et al. Distortions of the Mitral Valve in Acute Ischemic Mitral Regurgitation. *Ann Thorac Surg.* 1997;64:1026-1031
20. Levine RA, Hung J. Ischemic mitral regurgitation, the dynamic lesion: clues to the cure. *J Am Coll Cardiol.* 2003;42:1929-1932
21. Grosberg A, Gharib M, Kheradvar A. Effect of Fiber Geometry on Pulsatile Pumping and Energy Expenditure. *Bull Math Biol.* 2009;71:1580-1598
22. Kilner PJ, Yang G-Z, Wilkes AJ, Mohiaddin RH, Firmin DN, Yacoub MH. Asymmetric redirection of flow through the heart. *Nature.* 2000;404:759-761
23. Narula J, Vannan MA, DeMaria AN. Of That Waltz in My Heart. *J Am Coll Cardiol.* 2007;49:917-920

24. Bertini M, Sengupta PP, Nucifora G, Delgado V, Ng ACT, Marsan NA, et al. Role of Left Ventricular Twist Mechanics in the Assessment of Cardiac Dyssynchrony in Heart Failure. *J Am Coll Cardiol Img.* 2009;2:1425-1435
25. Mangual J, Jung B, Ritter J, Kheradvar A. Modeling Radial Viscoelastic Behavior of Left Ventricle Based on MRI Tissue Phase Mapping. *Annals of Biomedical Engineering.* 38:3102-3111
26. Kheradvar A, Milano M, Gorman R, Gorman J, Gharib M. Assessment of Left Ventricular Viscoelastic Components Based on Ventricular Harmonic Behavior. *Cardiovascular Engineering.* 2006;6:30-39
27. Kheradvar A. Development and Testing a Dynamic Bi-leaflet Mitral Prosthesis. *Circulation.* 2009;120:S929
28. Berdajs D, Zünd G, Camenisch C, Schurr U, Turina MI, Genoni M. Annulus Fibrosus of the Mitral Valve: Reality or Myth. *J Card Surg.* 2007;22:406-409
29. Ogden RW. Large Deformation Isotropic Elasticity - On the Correlation of Theory and Experiment for Incompressible Rubberlike Solids. *Proc R Soc Lond A.* 1972;326:565-584
30. May-Newman K, Yin FCP. A constitutive law for mitral valve tissue. *J Biomech Eng.* 1998;120:38-47
31. Weinberg EJ, Kaazempur Mofrad MR. A finite shell element for heart mitral valve leaflet mechanics, with large deformations and 3D constitutive material model. *J Biomech.* 2007;40:705-711
32. Falahatpisheh A, Kheradvar A. High-Speed Particle Image Velocimetry to Assess Cardiac Fluid Dynamics in vitro: From Performance to Validation. *Eur J Mech B-Fluids.* 2012;DOI:10.1016/j.euromechflu.2012.01.019
33. Klues HG, Proschan MA, Dollar AL, Spirito P, Roberts WC, Maron BJ. Echocardiographic assessment of mitral valve size in obstructive hypertrophic cardiomyopathy. Anatomic validation from mitral valve specimen. *Circulation.* 1993;88:548-555
34. Timek TA, Lai DT, Dagum P, Liang D, Daughters GT, Ingels NB, et al. Mitral leaflet remodeling in dilated cardiomyopathy. *Circulation.* 2006;114:I518-I523
35. Pedrizzetti G, Domenichini F, Tonti G. On the Left Ventricular Vortex Reversal after Mitral Valve Replacement. *Ann Biomed Eng.* 2010;38:769-773
36. Shariff K, Leonard A. Vortex Rings. *Annu Rev Fluid Mech.* 1992;24:U235-U79
37. Kheradvar A, Kasalko J, Johnson D, Gharib M. An In Vitro Study of Changing Profile Heights in Mitral Bioprostheses and Their Influence on Flow. *ASAIO J.* 2006;52:34-38
38. Krueger PS, Gharib, M. The significance of vortex ring formation to the impulse and thrust of a starting jet. *Phys Fluids.* 2003;15:1271-1281
39. Dabiri JO, Gharib M. Fluid entrainment by isolated vortex rings. *J Fluid Mech.* 2004;511:311-331